Supporting Information

Obeid et al. 10.1073/pnas.1013804107

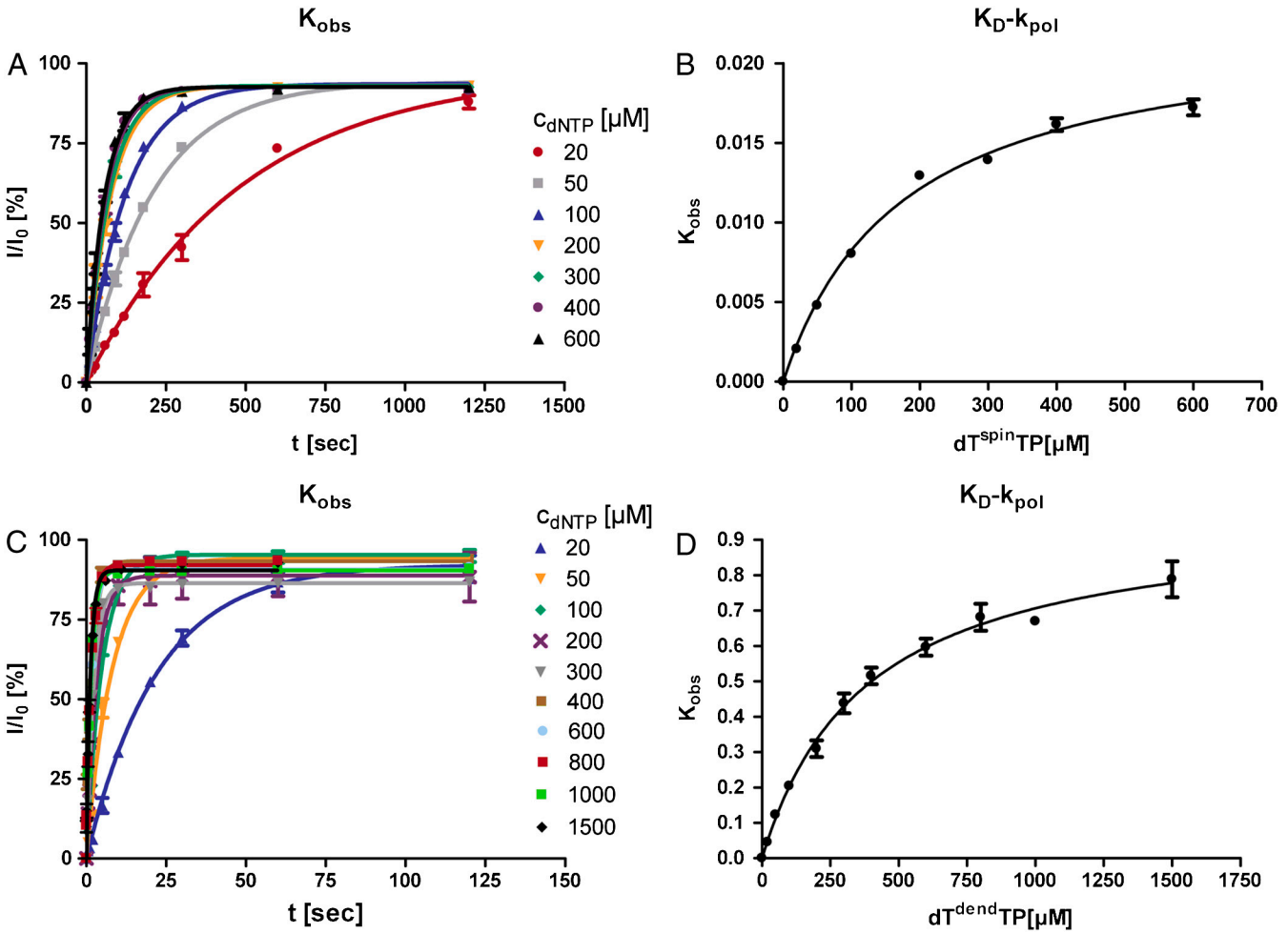

Fig. S1. Pre-steady-state kinetics of the modified $dT^{R}TP$. (*A*) Kinetics of single nucleotide incorporation opposite A catalyzed by *KlenTaq* in dependence of time and dNTP concentration. The single turnover is plotted against the time for various $dT^{spin}TP$ concentrations in µM (color code on the right side). (*B*) The curve show dependence of the observed pre-steady-state rates (k_{obs}) on $dT^{spin}TP$ concentration and fitted to a hyperbolic equation. (*C*) The same as *A* using $dT^{dend}TP$ instead of $dT^{spin}TP$. (*D*) The k_{obs} values were plotted versus the concentration of the used $dT^{dend}TP$ and fitted to a hyperbolic equation.

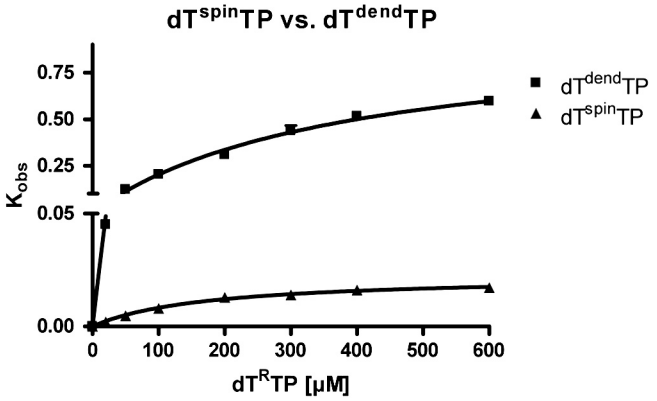

Fig. S2. Comparison of the pre-steady-state kinetics of the two modified dT^{R}TP. Pre-steady-state kinetics of single nucleotide incorporation opposite A catalyzed by *KlenTaq* wild type. The k_{obs} values were plotted versus the concentration of the used dT^{spin}TP (triangle) and dT^{dend}TP (square) and fitted to a hyperbolic equation, respectively.

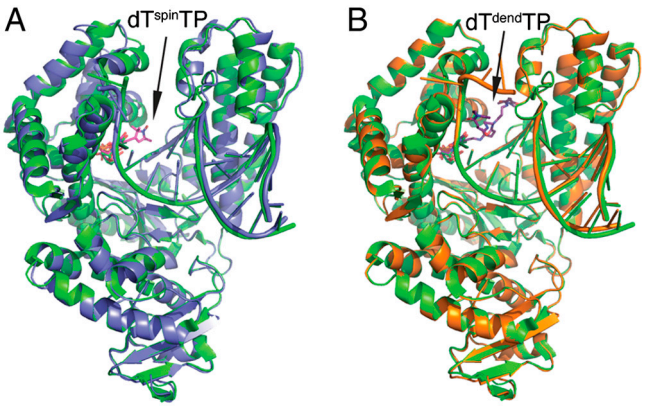

Fig. S3. Structure of *KlenTaq* in complex with C5 modified dT^{R}TPs. (*A*) Overall structure of *KlenTaq*$_{spin}$ (blue) is superimposed with ddTTP-trapped *KlenTaq* (1QTM, green). The location of dT^{spin}TP is indicated. (*B*) Overall structure of *KlenTaq*$_{dend}$ (orange) is superimposed with ddTTP-trapped *KlenTaq* (1QTM, green). The location of dT^{dend}TP is indicated.

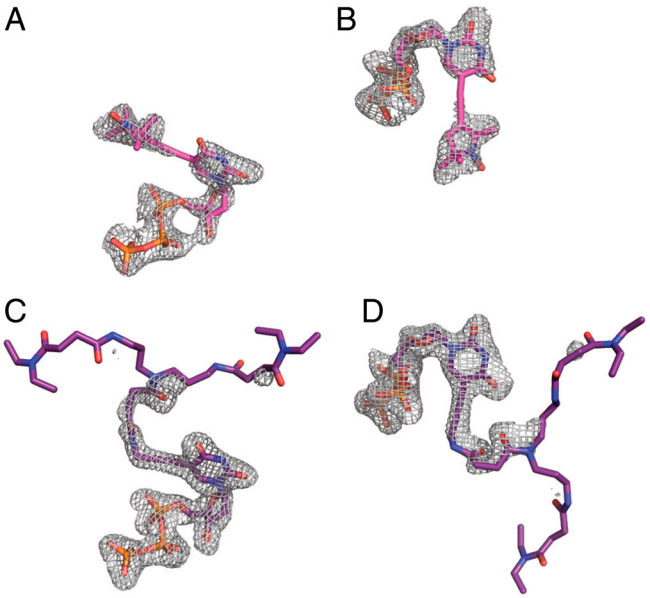

Fig. S4. Simulated annealing omit maps of the incoming dT^{R}TP. (*A* and *B*) The final refined simulated annealing omit map mFo-DFc at 3σ is shown for dT^{spin}TP. (*C* and *D*) The final refined simulated annealing omit map mFo-DFc encountered at 3σ is shown for dT^{dend}TP.

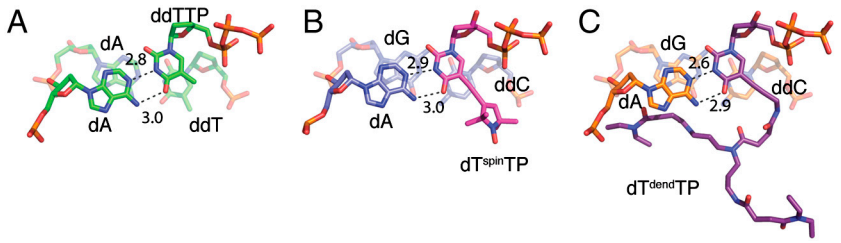

Fig. S5. Top view of the nascent base pair. (*A*) The nascent base pair of *KlenTaq* (PDB 1QTM). The hydrogen bonding between the incoming ddTTP and the templating dA is shown in dashed lines. In transparent the first nucleobase pair of the primer template terminus is shown. (*B*) The nascent base pair of *KlenTaq*$_{spin}$. The Watson–Crick base pairing interaction between the incoming dT^{spin}TP and the templating dA is shown in dashed lines. In transparent the first nucleobase pair of the primer template terminus is shown. (*C*) The nascent base pair of *KlenTaq*$_{dend}$. The interaction network between the incoming dT^{dend}TP and the templating dA is shown in dashed lines. In transparent the first nucleobase pair of the primer template terminus is shown.

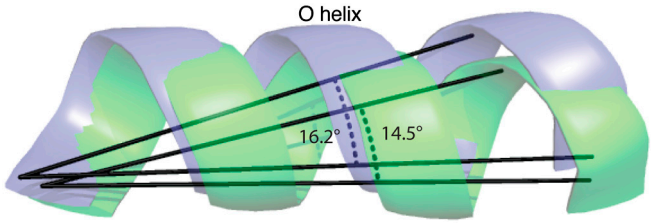

Fig. S6. Comparison of the O helices from *KlenTaq*$_{spin}$ and *KlenTaq* 1QTM. The O helices of the superimposed *KlenTaq*$_{spin}$ (blue) and ddTTP-trapped *KlenTaq* (green) structure are shown. The respective angle of the O helices are indicated.

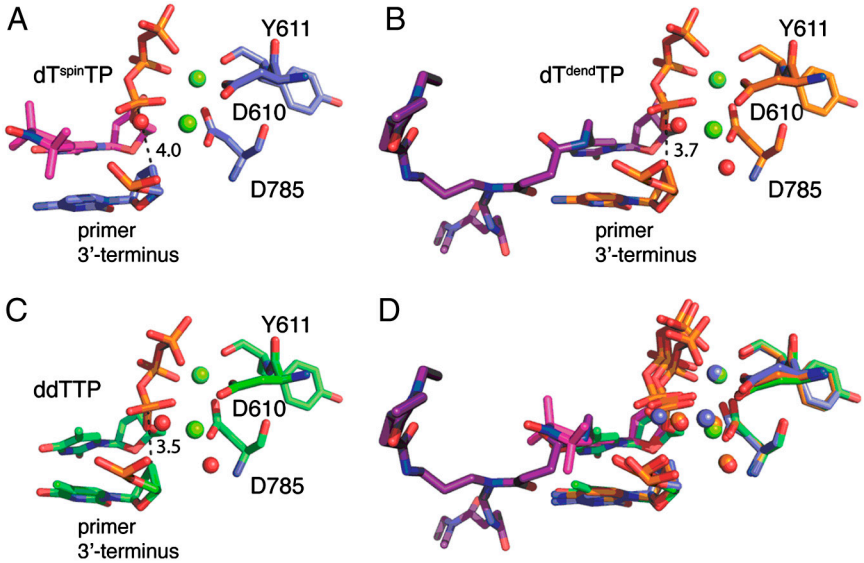

Fig. S7. Close-up views on the primer 3′-terminus, incoming nucleotide and amino acids complexing divalent cations. (*A*) Stick model derived from *KlenTaq*$_{spin}$. The distance of the α-phosphate from the incoming dT^{spin}TP to the primer 3′-terminus is 4.0 Å (highlighted in dashed lines). Water molecules (red) and magnesium ions (green) are indicated as spheres. (*B*) Same as in *A* for *KlenTaq*$_{dend}$. (*C*) Same as in *A* for the reported *KlenTaq*$_{1QTM}$. (*D*) Superpostion of structures depicted in *A*–*C* using the respective color code for the water and magnesium ions as well.

```
Thermus aquaticus                659 RRAAKTINFGVLYG 672
Thermus thermophilus             661 RRAAKTVNFGVLYG 674
Thermus filiformis               659 RRAAKTVNFGVLYG 672
Deinococcus radiodurans          784 RRAAKTVNFGVLYG 797
Escherichia coli (K12)           754 RRSAKAINFGLIYG 767
Haemophilus influenzae           757 RRNAKAINFGLIYG 770
Streptococcus pneumoniae         715 RRNAKAVNFGVVYG 728
Mycobacterium tuberculosis       729 RRRVKAMSYGLAYG 742
Mycobacterium leprae             736 RRRVKAMSYGLAYG 749
Treponema pallidum               823 RRIAKTINFGIVYG 836
Borrelia burgdorferi             734 RRIAKSINFGIIYR 746
Lactococcus lactis               703 RRNAKAVNFGVVYG 716
Rickettsia typhi                 700 RRKAKAINFGIIYG 713
Streptomyces coelicolor          732 RRKIKAMSYGLAYG 745
```

Fig. S8. Amino acid sequence alignment of DNA polymerases highlighting the conserved position equivalent to Arg660 in *KlenTaq*.

Table S1. Data collection and refinement statistics

	KlenTaq$_{spin}$ (PDB ID: 3OJU)	*KlenTaq*$_{dend}$ (PDB ID: 3OJS)
Data collection		
Space group	$P3_121$	$P3_121$
Cell dimensions		
a, *b*, *c* (Å)	109.0, 109.0, 91.5	107.8, 107.8, 90.2
α, β, γ (°)	90.0, 90.0, 120.0	90.0, 90.0, 120.0
Resolution (Å)	47.21 - 1.99 (2.11 - 1.99)*	46.69 - 1.90 (2.01 - 1.90)*
R_{meas}	10.8 (113.9)*	13.1 (154.6)*
$I/\sigma I$	16.7 (1.8)*	14.7 (1.6)*
Completeness (%)	74.5 (28.0)*	98.8 (93.7)*
Redundancy	10.6 (7.6)*	10.8 (8.9)*
Refinement		
Resolution (Å)	47.22 - 2.00 (2.06 - 2.00)*	46.71 - 1.90 (1.94 - 1.90)*
No. reflections	32113 (856)*	47553 (2333)*
R_{work}/R_{free}	17.7/21.9 (22.3/25.6)*	16.3/21.2 (25.8/28.2)*
No. atoms		
Protein	8612	8662
Ligand/ion	582/2	650/2
Water	195	332
B-factors		
Protein	49.9	47.7
Ligand/ion	41.1/42.0	44.1/30.7
Water	40.0	45.1
R.m.s. deviations		
Bond lengths (Å)	0.004	0.006
Bond angles (°)	1.060	1.120

*Values in parentheses are for highest-resolution shell.